Supporting information

Chemistry

LCMS was performed using an Agilent 1100 HPLC systems with an XBridge 3.5 µm C18 column (100 x 4.60 mm) coupled to a Hewlett Packard 1100 series mass spectrometer with an electrospray ionization source, operating with 1.0 mL/min over 10 min using a gradient consisting of eluent A (H_2O:CH_3CN:HCOOH, 95:5:0.1) and eluent B (H_2O:CH_3CN:HCO_2H, 5:95:0.05). Gradient: 0–100% eluent B over 8 min. NMR-spectra were acquired using a 400 MHz Bruker Avance III equipped with a 5 mm broad band probe (BBFO) and a 600 MHz Bruker Avance III HD equipped with a cryogenically cooled 5 mm dual probe optimized for ^{13}C and ^{1}H. ^{1}H-NMR spectra were recorded at 400.09 MHz using 30°-pulses, a spectral width of 8 kHz, collecting 16 scans with a length of 65536 data points and with a relaxation delay of 1.0 sec. FID's were zero-filled to twice the size and exponentially multiplied with a line broadening factor of 0.3 Hz before Fourier transformation. ^{13}C-NMR spectra were acquired at 100.60 MHz with 30°-pulses, a spectral width of 24 kHz, collecting 256 scans with a length of 65536 data points and with a relaxation delay of 2.0 sec. The ^{13}C nuclei were ^{1}H-decoupled using the Waltz-16 composite pulse decoupling scheme. FID's were exponentially multiplied with a line broadening factor of 1.0 Hz before Fourier transformation. Analytical HPLC was performed on a system consisting of an Ultimate 3000 pump and PDA detector, and a TSP AS-3000 autosampler with a Gemini-NX C_{18} column (4.6 mm × 250 mm) or on an Agilent 1260 system with Innoval C_{18} column (4.6 mm × 250 mm) equipped with a 254 nm UV detector using a linear gradient elution of the binary solvent system of H_2O/MeCN/TFA (v/v/v; A: 95/5/0.1, and B: 5/95/0.1) with the concentration of B from 0% to 100% over 20 min with a flow rate of 1.0 mL/min. Preparative HPLC for the purification of final compounds was performed on an Ultimate 3000 system with a Gemini-NX C_{18} column (21 mm × 250 mm) or on a Waters instrument with an Innoval C_{18} column (21.2 mm × 250 mm) equipped with a 254 nm UV detector with the same binary solvent system with a flow rate of 20 mL/min. Purities of the tested compounds were determined by analytical HPLC to be > 95%. Identity was confirmed by NMR and LCMS showing the correct mass.

*General procedure for compound **7**–**10b*** and ***11b**–**12b***.

To a dispersion of NaH (60% in mineral oil, >2 equiv) was added *N*-Boc serine in anhydrous DMF at 0 °C. The reaction was stirred for 10-60 min and the alkyl halide was then added (1.2–2.4 equiv). The reaction was stirred 4–20 h as judged by TLC, then quenched with sat. NH_4Cl (1 mL) and the mixture was partioned between Et_2O (20 mL) and icecold 0.1 M HCl (10 mL). The aqueous phase was extracted with Et_2O (3 x 50 mL), dried ($MgSO_4$), concentrated and purified by column chromatography (Eluent 0-100 % EtOAc in hexane, 1 % CH_3CO_2H). The purified product was then deprotected using HCl (2M in Et_2O, 20 equiv) or by adding TFA (20 equiv) in CH_2Cl_2. The compounds were purified by precipitation from EtOH/Et_2O and/or by preparative HPLC.

(*R*)-*O*-Butylserine (**7**). Following the general procedure, compound **7** was synthesized from 1-bromobutane and was obtained as the HCl salts (yield: 17%, 2 steps). ^{1}H NMR (400 MHz, Methanol-d_4) δ 4.19 (dd, J = 4.8, 3.3 Hz, 1H), 3.92 (dd, J = 10.5, 4.8 Hz, 1H), 3.85 (dd, J = 10.5, 3.3 Hz, 1H), 3.67 – 3.47 (m, 2H), 1.72 – 1.53 (m, 2H), 1.42 (ddt, J = 14.5, 9.6, 7.4 Hz, 2H), 0.96 (t, J = 7.4 Hz, 3H). ^{13}C NMR (151 MHz, Methanol-d_4) δ 169.8, 72.5, 68.8, 54.4, 32.5, 20.2, 14.2. MS calcd for $C_7H_{15}NO_3H^+$ $[M+H]^+$: 162.1, found: 161.9. Mp: >300 °C.

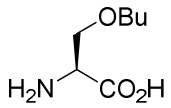

(*R*)- and (*S*)-*O*-Benzylserine (**8a**, **8b**). Following the general procedure, compound **8a** and **8b** were synthesized from benzylbromide and were obtained as the HCl salts (yield: 21%, 2 steps for **8a** and 31%, 2 steps for **8b**).

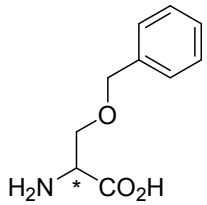

Analytical data for **8a:** ^{1}H NMR (300 MHz; Methanol-d_4): δ 7.36-7.29 (m, 5H), 4.66-4.56 (m, 2H), 4.17 (dd, J = 4.8, 3.3 Hz, 1H), 3.88 (qd, J = 11.5, 4.1 Hz, 2H). ^{13}C NMR (75 MHz; Methanol-d_4): δ 169.7, 138.4, 129.3, 128.91, 128.89, 74.4, 68.2, 54.4. MS calcd for $C_{10}H_{13}NO_3H^+$ $[M+H]^+$:196.1, found: 196.1. Mp: 193.3–194.3 °C.

Same data was found for **8b**.

(*R*)- and (*S*)-*O*-(naphthalen-2-ylmethyl)serine (**9a**, **9b**). Following the general procedure, compound **9a** and **9b** were synthesized from 2-(bromomethyl)naphthalene and were obtained as the HCl salts (yield: 63%, 2 steps for **9a** and 21%, 2 steps for **9b**).

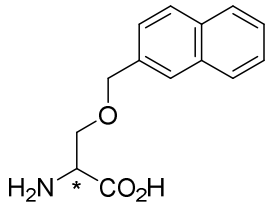

Analytical data for **9a:** ^{1}H NMR (400 MHz, Methanol-d_4) δ 7.90 – 7.80 (m, 4H), 7.53 – 7.42 (m, 3H), 4.80 (d, J = 12.2 Hz, 1H), 4.75 (d, J = 12.2 Hz, 1H), 4.22 (d, J = 4.2 Hz, 1H), 3.99 (dd, J = 10.5, 4.2 Hz, 1H), 3.92 (d, J = 10.5 Hz, 1H). ^{13}C NMR (101 MHz, Methanol-d_4) δ 169.7, 136.0, 134.7, 134.6, 129.2, 128.9, 128.7, 127.8, 127.2, 127.1, 126.8, 74.5, 68.3, 54.4. MS calcd for $C_{14}H_{15}NO_3H^+$ $[M+H]^+$: 246.1, found: 246.1.

Same data was found for **9b**.

(*R*)- and (*S*)-*S*-Butylcysteine (**10a**, **10b**). Following the general procedure, compound **10a** and **10b** were synthesized from 1-bromobutane and were obtained as the HCl salts (yield: 23%, 2 steps for **10a** and 47% yield, 2 steps for **10b**).

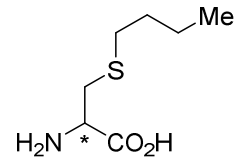

Analytical data for **10a:** ^{1}H NMR (400 MHz, Methanol-d_4) δ 4.18 (dd, J = 7.4, 4.4 Hz, 1H), 3.15 (dd, J = 14.7, 4.4 Hz, 1H), 3.04 (dd, J = 14.4, 7.4 Hz 1H), 2.63 (td, J = 7.4, 2.6 Hz, 2H), 1.61 (p, J = 7.4 Hz, 2H), 1.45 (h, J = 7.4 Hz, 2H), 0.95 (t, J = 7.4 Hz, 3H). ^{13}C NMR (101 MHz, Methanol-d_4) δ 170.7, 53.7, 33.14, 33.06, 32.7, 23.0, 14.2. MS calcd for $C_7H_{15}NO_2SH^+$ $[M+H]^+$: 178.1, found: 178.1. Mp: 209.9–215 °C.

Same data was found for **10b**.

(*R*)- and (*S*)-*S*-Benzylcysteine (**11a**, **11b**). Synthesis of **11a**: To Boc-cysteine (400 mg, 1.82 mmol) in anhydrous DMF (10 mL) was added K_2CO_3 (630 mg, 4.55 mmol, 2.5 equiv) followed by bromomethylbenzene (230 µL, 1.9 mmol, 1.04 equiv). The reaction was stirred for 16 h, then quenched with 1M $KHSO_4$ (60 mL) and extracted with EtOAc (3 x 50 mL). The combined organic phases were washed with brine (4 x 30 mL), dried ($MgSO_4$) and concentrated. For deprotection, the purified compound was dissolved in 2 M HCl in Et_2O (20 equiv) and stirred for 16 h. The final product was obtained as a white solid (yield: 16 % yield, 2 steps). Following the general procedure, compound **11b** was synthesized from bromomethylbenzene and obtained as the HCl salt (yield: 7%, 2 steps).

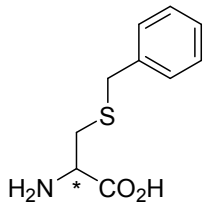

Analytical data for **11a:** ^{1}H NMR (600 MHz, Methanol-d_4) δ 7.39 – 7.36 (m, 2H), 7.35 – 7.31 (m, 2H), 7.29 – 7.25 (m, 1H), 4.09 (dd, J = 8.1, 4.1 Hz, 1H), 3.84 (s, 2H), 3.06 (dd, J = 14.8, 4.1 Hz, 1H), 2.91 (dd, J =

14.8, 8.1 Hz, 1H). ^{13}C NMR (151 MHz, Methanol-d_4) δ 169.1, 137.3, 128.8, 128.3, 127.1, 51.8, 35.5, 30.8. MS calcd for $C_{10}H_{13}NO_2SH^+$ $[M+H]^+$: 212.1, found: 212.1. Mp: 209.9–210.5 °C.

Same data was found for **11b**.

(*R*)- and (*S*)-*S*-(naphthalen-2-ylmethyl)cysteine (**12a**, **12b**). Following the general procedure, compound **12a** and **12b** were synthesized from 2-(bromomethyl)naphtalene and were obtained as the HCl salts (yield: 8%, 2 steps for **10a** and 5% yield, 2 steps for **10b**).

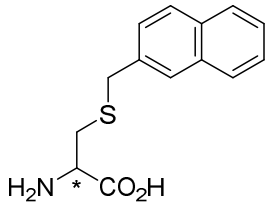

Analytical data for **12a:** ^{1}H NMR (600 MHz, DMSO-d_6) δ 7.88 (dd, J = 8.0, 3.6 Hz, 2H), 7.86 – 7.84 (m, 1H), 7.84 – 7.82 (m, 1H), 7.54 – 7.47 (m, 3H), 3.96 (d, J = 5.2 Hz, 2H), 3.83 (s, 1H), 2.90 (dd, J = 14.3, 4.4 Hz, 1H), 2.80 (dd, J = 14.3, 7.5 Hz, 1H). ^{13}C NMR (151 MHz, DMSO) δ 169.6, 136.0, 133.2, 132.5, 128.6, 128.02, 127.97, 127.8, 127.8, 126.8, 126.3, 52.8, 35.8, 32.0. MS calcd for $C_{14}H_{14}NO_2SH^+$ $[M+H]^+$: 261.1, found: 262.2. Mp: 123.6–126.3 °C. Mp: 208.7–214.0 °C.

Same data was found for **12b**.

(*R*)- and (*S*)-2-Amino-3-pentanamidopropanoic acid (**13a**, **13b**). To Boc-aminopropanoic acid (0.5 g, 2.4 mmol) in anhydrous THF (5 mL) was added DIPEA (2.1 mL, 12.2 mmol, 5 equiv) and pentanoyl chloride (0.3 mL, 2.4 mmol, 1 equiv). The mixture was stirred at room temperature 16 h, then diluted with H_2O (10 mL), where after 1 M HCl was added (until pH=2-3). The mixture was extracted with EtOAc (2 x 20 mL), washed with brine (2 x 10 mL), dried (MgSO4) and evaporated. For deprotection, the purified compound was dissolved in 2 M HCl in Et_2O and stirred for 2.5 h. The final product was obtained as a yellow sticky solid (yield: 35%, 2 steps for **13a** and 26%, 2 steps for **13b**).

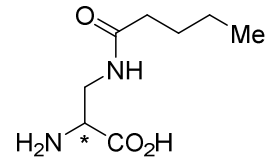

Analytical data for **13a:** ^{1}H NMR (400 MHz, DMSO-d_6) δ 8.46 (brs, 3H), 8.26 (t, J = 5.8 Hz, 1H), 3.99 – 3.90 (m, 1H), 3.61 – 3.43 (m, 2H), 2.10 (t, J = 7.5 Hz, 2H), 1.47 (p, J = 7.4 Hz, 2H), 1.25 (h, J = 7.3 Hz, 2H), 0.85 (t, J = 7.3 Hz, 3H); ^{13}C NMR (151 MHz, DMSO) δ 173.4, 169.1, 52.4, 38.6, 34.9, 27.1, 21.7, 13.7. MS calcd for $C_8H_{16}N_2O_3H^+$ $[M+H]^+$: 189.1, found: 188.9.

Same data was found for **13b**.

(*R*)- and (*S*)-2-Amino-3-benzamidopropanoic acid (**14a**, **14b**). To Boc-aminopropanoic acid (0.5 g, 2.4 mmol) in anhydrous THF (5 mL) was added DIPEA (2.1 mL, 12.2 mmol, 5 equiv) and benzoyl chloride (0.28 mL, 2.4 mmol, 1 equiv). The mixture was stirred at room temperature 16 h, then diluted with H_2O (10 mL, where after 1 M HCl was added (until pH=2-3). The mixture was extracted with EtOAc (2 x 20 mL), washed with brine (2 x 10 mL), dried (MgSO4) and evaporated. For deprotection, the purified compound was dissolved in 2 M HCl in Et_2O and stirred for 2.5 h. The final product was obtained as a white solid (yield: 23%, 2 steps for **14a** and 29%, 2 steps for **14b**).

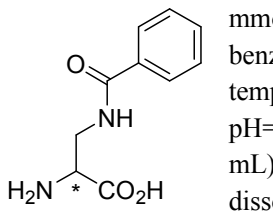

Analytical data for **14a:** ^{1}H NMR (400 MHz, DMSO-d_6) δ 8.82 (t, J = 5.8 Hz, 1H), 8.46 (brs, 3H), 7.91 (d, J = 7.5 Hz, 2H), 7.56 (t, J = 7.5 Hz, 1H), 7.49 (t, J = 7.5 Hz, 2H), 4.15 – 4.10 (m, 1H), 3.84 – 3.70 (m, 2H);

^{13}C NMR (151 MHz, Methanol-d_4) δ 171.7, 169.9, 134.7, 133.2, 129.6, 128.6, 54.9, 41.1. MS calcd for $C_{10}H_{12}N_2O_3H^+$ $[M+H]^+$:209.1, found: 208.9.

Same data was found for **14b**.

(*R*)- and (*S*)-3-(2-Naphthamido)-2-aminopropanoic acid (**15a**, **15b**). To Boc-aminopropanoic acid (0.5 g, 2.4 mmol) in anhydrous THF (5 mL) was added DIPEA (2.1 mL, 12.2 mmol, 5 equiv) and 2-naphthoyl chloride (0.46 g, 2.4 mmol, 1 equiv). The mixture was stirred at room temperature 16 h, then diluted with H_2O (10 mL), where after 1 M HCl was added (until pH=2-3). The mixture was extracted with EtOAc (2 x 20 mL), washed with brine (2 x 10 mL), dried (MgSO4) and evaporated. For deprotection, the purified compound was dissolved in 2 M HCl in Et_2O and stirred for 2.5 h. The final product was obtained as a white solid (yield: 25%, 2 steps for **15a** and 30%, 2 steps for **15b**).

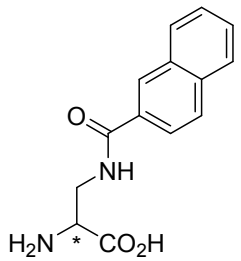

Analytical data for **15a:** ^{1}H NMR (400 MHz, DMSO-d_6) δ 13.89 (s, 1H), 8.99 (t, J = 5.8 Hz, 1H), 8.53 (s, 1H), 8.48 (brs, 3H), 8.03 – 7.94 (m, 4H), 7.70 – 7.53 (m, 2H), 4.14 (t, J = 5.8 Hz, 1H), 3.94 – 3.71 (m, 2H). ^{13}C NMR (151 MHz, DMSO) δ 169.1, 166.9, 134.2, 132.0, 131.0, 128.8, 128.0, 127.8, 127.73 127.6, 126.8, 124.3, 52.4, 39.4. MS calcd for $C_{14}H_{14}N_2O_3H^+$ $[M+H]^+$: 259.1, found: 259.1. Mp: 226.3-232.4°C.

Same data was found for **15b**.

(*R*)- and (*S*)-2-Amino-3-(4,7-dichloro-1H-indole-2-carboxamido)propanoic acid (**16a**, **16b**). To 4,7-dichloro-1H-indole-2-carboxylic acid (0.3 g, 1.3 mmol) in THF (5 mL) was added 2 M oxalylchloride in CH_2Cl_2 (1.3 mL, 2.6 mmol, 2 equiv) and a drop of DMF. The reaction was stirred at room temperature for 1 h and then concentrated. The crude material was redissolved in THF (5 mL), where after To Boc-aminopropanoic acid (0.27 g, 1.3 mmol, 1 equiv) and DIPEA (1.1 mL, 6.5 mmol, 5 equiv) was added. The mixture was stirred at room temperature 1 h, then diluted with H_2O (10 mL) and 1 M HCl (2 mL, to pH = 2-3) and extracted with EtOAc (2 x 20 mL). The combined organic phases were washed with brine (2 x 10 mL), dried ($MgSO_4$), and concentrated. For deprotection, the purified compound was dissolved in 2 M HCl in Et_2O and stirred for 2.5 h. The final product was obtained as a white solid (yield: 9%, 3 steps for **16a** and 12%, 3 steps for **16b**).

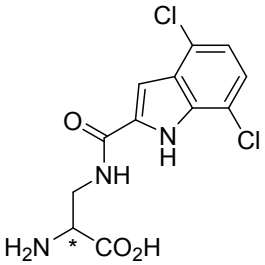

Analytical data for **16a:** ^{1}H NMR (600 MHz, DMSO-d_6) δ 13.99 (brs, 1H), 12.22 (s, 1H), 9.04 (t, J = 5.8 Hz, 1H), 8.42 (brs, 3H), 7.32 (d, J = 8.1 Hz, 1H), 7.31 (d, J = 1.8 Hz, 1H), 7.18 (d, J = 8.1 Hz, 1H), 4.13 – 4.09 (m, 1H), 3.84 (dt, J = 14.3, 5.2 Hz, 1H), 3.78 – 3.72 (m, 1H). ^{13}C NMR (151 MHz, DMSO) δ 169.0, 160.5, 134.0, 133.7, 126.8, 124.4, 124.0, 120.4, 115.8, 104.1, 52.3, 38.9. MS calcd for $C_{12}H_{11}Cl_2N_3O_3H^+$ $[M+H]^+$: 316.0, found: 316.0. Mp: 218.7-224.8°C.

Same data was found for **16b**.

Molecular Modeling

Analyses of crystal structures.

The cavity extending from the glycine binding pocket in GluN1 into the GluN1-GluN2 ABD dimer interface was detected using the CAVER 3.0.1 plugin[1] for the PyMOL Molecular Graphics System, Version 1.8 Schrödinger, LLC. Briefly, the glycine agonist bound in the GluN1/2A ABD dimer crystal structure (PDB: 5I57) was selected as starting point and the cavity was detected using default parameters.

Ligand-docking and molecular dynamics simulations.

The starting structure for the GluN1/2A models was built primarily from the PDB ID: 5I59 crystal structure, with missing loops built by extracting and adding residues from PDB ID: 5I56, and then using the SwissModel server (https://swissmodel.expasy.org/) to fill remaining gaps and missing side chains. Compound **15a** was then docked into the glycine binding site of the GluN1 subunit in the starting structure using the GOLD docking program (https://www.ccdc.cam.ac.uk) with side chains expected to line the binding cavity allowed to be flexible (Figure S2). Furthermore, bound glycine from PDB ID: 5I59 crystal structure was used as reference for the amino acid moiety of compound **15a**. The two highest-scored **15a** poses using the ChemScore scoring algorithm, as well as the ligands glycine and glutamate from the PDB ID: 5I59 crystal structure, were parameterized using the Antechamber program included in AmberTools 16 for inclusion in subsequent molecular dynamics simulations.

The resulting GluN1/2A models with either bound glycine/glutamate or bound **15a**/glutamate were solvated with approximately 25,800 TIP3P water molecules in a truncated octahedron bounding box with a minimum of 12 Å buffer region between the solute and the edge of the unit cell. The system was then ionized to 150 mM NaCl by adding 72 sodium ions and then adding 75 chlorine ions to neutralize the system. Using the Generalized Amber Force Field included with Amber16 (ff14SB)[2] the solvated and ionized systems were energy minimized (steepest descent, 2000 iterations), slowly heated to 310 K over 300 ps under constant volume and temperature (NVT) conditions, and equilibrated under constant pressure and temperature (NpT) conditions (pressure at 1 atm) for 1 ns, with gradually reduced restraints on heavy atoms. Restraints were reduced at 200 ps intervals from 5 kcals/mol to 3 kcals/mol, then to 2 kcals/mol and then halved until 0.5 kcals/mol, which was followed by 100 ps of unrestrained molecular dynamics under NpT conditions. Production simulations of the equilibrated molecular systems were run for 300 ns under NpT conditions, with a total of four simulations for the glycine/glutamate-bound systems, and four simulations for the **15a**/glutamate-bound systems (two simulations for each of the docked poses of **15a**). Periodic boundary conditions were applied to all simulations with the particle mesh Ewald method used to calculate long-range electrostatic interactions and with a cutoff beyond 8 Å for electrostatic calculations. The Monte Carlo barostat method was used to achieve constant pressure, and the Langevin dynamics method was used to achieve constant temperature (310 K). To allow for integration time steps of 4 fs, the SHAKE algorithm was used to constrain hydrogen bonds, while the mass of solute hydrogen atoms was repartitioned to a new hydrogen mass of 3.024 daltons, with subsequent adjustment of the mass to which each hydrogen is bonded to the amount necessary to leave total mass unchanged. To evaluate hinged movement between GluN1 lobes that form the agonist binding cleft, distances were measured between the centers of mass (calculated using AmberTools 16) for atoms N, CA, CB, C, and O of residues 484–485 in GluN1 lobe 1 and residues 688-689 in GluN1 lobe 2 (distance ξ_1), and between residues 405-407 in GluN1 lobe 1 and residues 714-715 in GluN1 lobe 2 (distance ξ_2) as previously described (Figure S3).[3]

Figure S1. Evaluation of **10a**, **11a**, and **12a** as competitive antagonists at the glycine binding site.

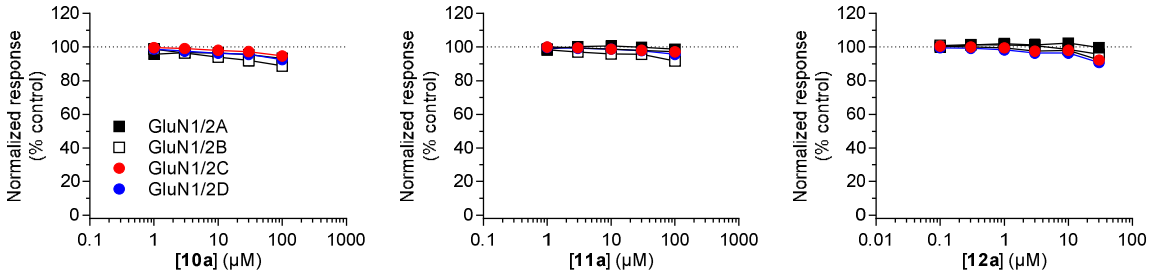

Concentration-inhibition data at NMDA receptor subtypes (GluN1/2A-D) expressed in *Xenopus* oocytes were measured using two-electrode voltage-clamp recordings. The NMDA receptors were activated by 3 μM glycine plus 300 μM glutamate in the absence and presence of increasing compound concentrations. None of the compounds produced marked inhibition of NMDA receptor responses, demonstrating that these ligands are not high-affinity competitive antagonists at the glycine binding site.

Figure S2. Ligand-docking poses of **15a** in the GluN1/2A ABD dimer structure.

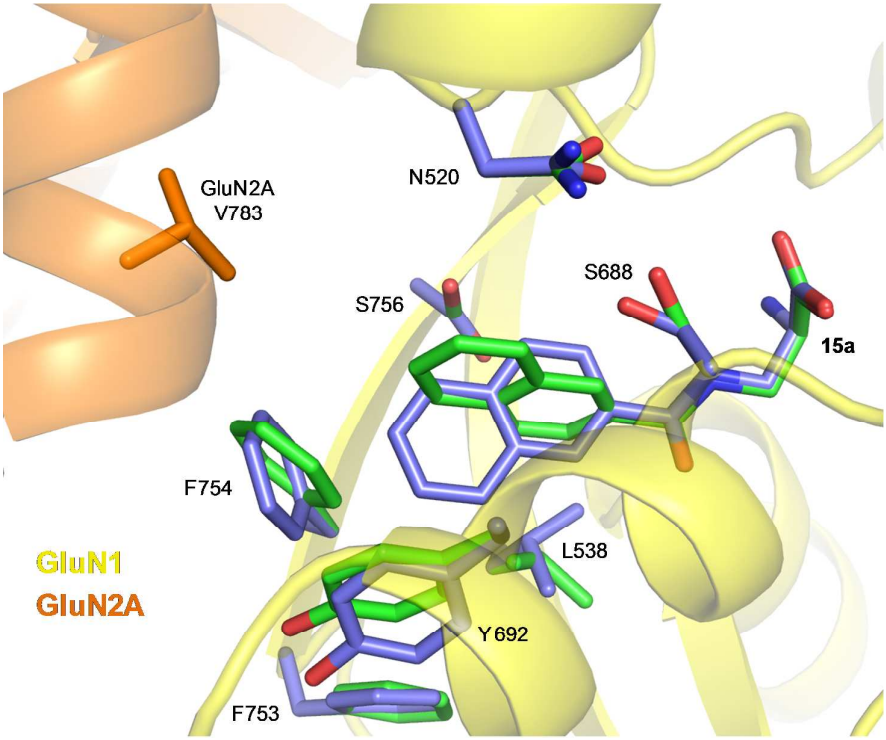

Compound **15a** docked into the glycine binding site of the GluN1 subunit in a GluN1/2A ABD dimer model built from PDB ID: 5I59. The GluN1 subunit is shown in yellow and the GluN2A subunit is shown in orange cartoon. The two highest scoring poses of **15a** obtained using the GOLD docking program (https://www.ccdc.cam.ac.uk) and the ChemScore scoring algorithm are shown in blue and green. Highlighted side chains in blue and green were flexible during ligand-docking simulations.

Figure S3. Global conformations of the GluN1 ABD during molecular dynamics simulations.

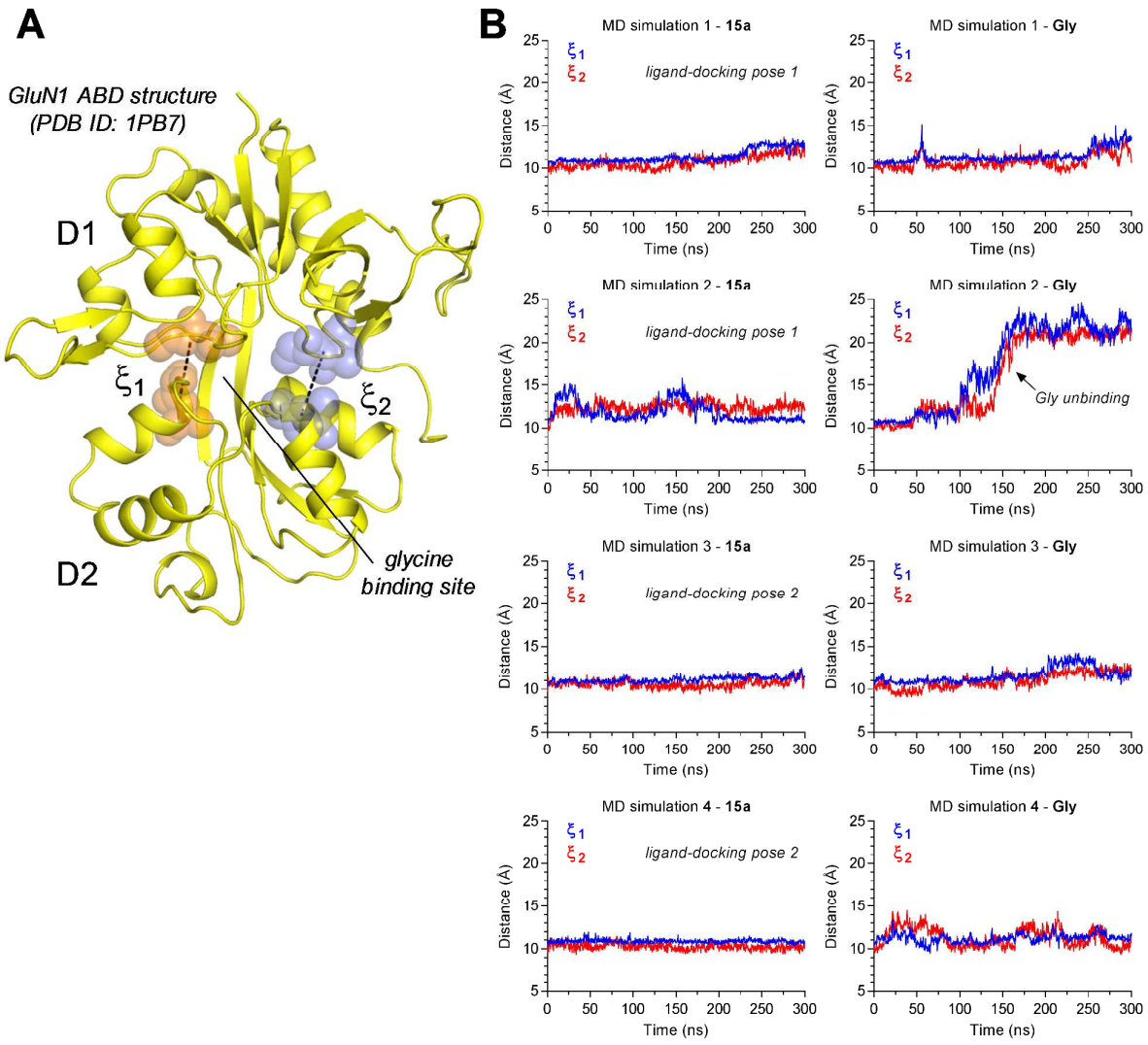

A) Crystal structure of the Gly-bound GluN1 ABD shown with two distances between the upper and lower lobes of the ABD (D1 and D2). Agonists bind the cleft formed between D1 and D2. ξ_1 and ξ_2 represent the distances between centers of mass for atoms N, CA, CB, C, and O (shown as spheres) of residues 484–485 in GluN1 D1 and residues 688-689 in GluN1 D2 (ξ_1), and between residues 405-407 in GluN1 D1 and residues 714-715 in GluN1 D2 (ξ_2). These distances have been used to describe closing or opening of the cleft in the ABD (i.e. shorter versus longer distances, respectively) in response to agonist binding or unbinding, and will report on global conformational changes in the GluN1 ABD.[3-5] B) Graphs with ξ_1 and ξ_2 distances during molecular dynamics simulations. Compound **15a** was docked into the glycine binding site of GluN1 in the GluN1/2A ABD dimer structure to obtain two initial high scoring poses (Figure S2) and four molecular dynamics simulations (300 ns each) were performed using these two poses (two simulations for each pose). For comparison, four molecular dynamics simulations (300 ns each) were performed with Gly bound in in the GluN1/2A ABD dimer structure. Gly dissociated from the GluN1 ABD in one of the four simulations, but with the exception of this simulation, binding of compound **15a** did not result in noticeable differences in the global conformation of the GluN1 ABD compared to binding of Gly.

Scheme S1. Synthetic routes to compounds **7-16**.

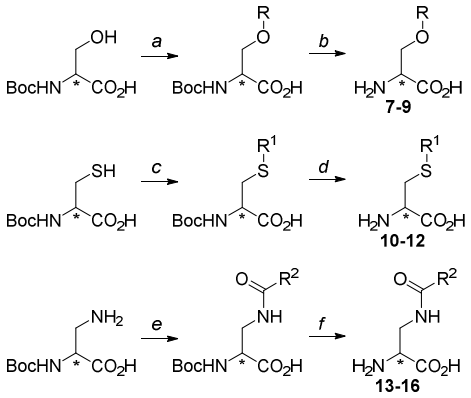

Reagents and conditions: a) NaH (60% in mineral oil), R-Cl/R-Br/R-I, DMF, 0 °C to rt. b) 2M HCl in Et2O or TFA in CH2Cl2, rt. c) K2CO3, R-Br, DMF, 0 °C to rt. d) 2M HCl in Et2O. e) R-COCl, DIPEA, THF. d) 2M HCl in Et2O.

Table S1. Agonist potencies and efficacies of compounds at recombinant GluN1/GluN2A-D receptors measured using TEVC electro-physiology. The relative maximal currents (R_{max}) are the maximal responses to the indicated agonists obtained by fitting the full concentration-response data normalized to the maximal response activated by glycine in the same recording. N indicates number of oocytes. Where full concentration-response data could not be determined, EC_{50} is indicated as >300. NR indicates responses <5 % at 300 μM of the compound.

	GluN1/2A					GluN1/2B					GluN1/2C					GluN1/2D				
	EC_{50} (μM)	pEC_{50} ± SEM	Hill slope	R_{max} (%) ± SEM	N	EC_{50} (μM)	pEC_{50} ± SEM	Hill slope	R_{max} (%) ± SEM	N	EC_{50} (μM)	pEC_{50} ± SEM	Hill slope	R_{max} (%) ± SEM	N	EC_{50} (μM)	pEC_{50} ± SEM	Hill slope	R_{max} (%) ± SEM	N
Gly (2)	0.95	6.033 ± 0.058	1.42	100	4	0.24	6.621 ± 0.008	1.59	100	4	0.20	6.709 ± 0.015	1.49	100		0.09	7.051 ± 0.009	1.48	100	4
D-Ser (3)	1.0	6.000 ± 0.018	1.60	96 ± 3	3	0.51	6.292 ± 0.028	1.31	98 ± 1	4	0.18	6.734 ± 0.011	1.37	119 ± 2	4	0.15	6.831 ± 0.047	1.35	95 ± 1	4
7	123	3.988 ± 0.139	1.30	36 ± 8	4	49	4.306 ± 0.016	1.05	61 ± 2	3	38	4.415 ± 0.005	1.26	91 ± 2	4	12	4.926 ± 0.001	1.55	69 ± 1	4
8a	95	4.024 ± 0.028	1.88	53 ± 3	4	40	4.394 ± 0.012	1.55	54 ± 1	6	21	4.676 ± 0.014	1.50	108 ± 1	6	14	4.840 ± 0.010	1.50	88 ± 1	6
8b	NR				4	>300				4	>300				4	>300				4
9a	NR				4	NR				4	45	4.352 ± 0.015	1.41	61 ± 1	4	94	4.027 ± 0.024	1.28	55 ± 1	1
9b	NR				4	NR				4	NR				4	NR				4
10a	NR				4	NR				4	>300				4	>300				4
10b	NR				4	>300				4	>300				4	>300				4
11a	NR				4	NR				4	87	4.060 ± 0.003	2.25	169 ± 5	4	>300				4
11b	NR				4	NR				4	>300				4	>300				4
12a	NR				3	NR				4	NR				4	NR				4
12b	NR				4	NR				4	>300				4	>300				4
13a	>300				4	>300				4	206	3.687 ± 0.005	1.33	223 ± 2	4	>300				4
13b	NR				4	NR				4	>300				4	>300				4
14a	84	4.080 ± 0.037	1.57	46 ± 1	4	56	4.253 ± 0.010	1.21	17 ± 1	4	38	4.416 ± 0.014	1.54	71 ± 2	4	115	3.949 ± 0.029	1.29	98 ± 2	8
14b	>300				4	>300				4	>300				4	>300				4
15a	12.3	4.916 ± 0.050	1.57	27 ± 2	3	3.83	5.421 ± 0.034	1.45	15 ± 1	4	1.97	5.705 ± 0.014	1.55	398 ± 17	4	20.1	4.698 ± 0.014	1.60	40 ± 1	4
15b	NR				3	NR				4	274	3.570 ± 0.049	1.67	148 ± 11	4	>300				4
16a	2.56	5.593 ± 0.019	1.45	13 ± 1	4	0.4	6.428 ± 0.033	1.98	5 ± 1	4	0.32	6.488 ± 0.010	1.95	308 ± 24	4	0.3	6.522 ± 0.014	2.04	8 ± 1	4
16b	NR				4	NR				4	93	4.034 ± 0.031	1.80	27 ± 1	4	NR				4

References

1. Chovancová, E.; Pavelka, A.; Beneš, P.; Strnad, O.; Brezovský, J.; Kozlíková, B.; Gora, A.; Šustr, V.; Klvaňa, M.; Medek, P.; Biedermannová, L.; Sochor, J.; Damborský, J. CAVER 3.0: A Tool for the Analysis of Transport Pathways in Dynamic Protein Structures, *PLoS Comput. Biol.* **2012***, 8*, e1002708.
2. Maier, J. A.; Martinez, C.; Kasavajhala, K.; Wickstrom, L.; Hauser K. E.; Simmerling C. ff14SB: Improving the Accuracy of Protein Side Chain and Backbone Parameters from ff99SB. *J. Chem. Theor. Comput.,* **2015**, *11*, 3696-3713.
3. Yao, Y.; Belcher, J.; Berger, A. J.; Mayer, M. L.; Lau, A. Y. Conformational analysis of NMDA receptor GluN1, GluN2, and GluN3 ligand-binding domains reveals subtype-specific characteristics. *Structure* **2013**, *21*,1788-1799.
4. Dai, J.; Zhou, H. X. Reduced curvature of ligand-binding domain free-energy surface underlies partial agonism at NMDA receptors. *Structure* **2015**, *23,* 228-236.
5. Dai, J., Zhou, H. X. Semiclosed Conformations of the Ligand-Binding Domains of NMDA Receptors during Stationary Gating. *Biophys. J.* **2016**, *111*, 1418-1428.